Electron Attachment to the Hydrogenated Watson−Crick Guanine Cytosine Base Pair (GC+H): Conventional and Proton-Transferred Structures

ARTICLE *in* THE JOURNAL OF PHYSICAL CHEMISTRY A · AUGUST 2008

Impact Factor: 2.69 · DOI: 10.1021/jp711958p · Source: PubMed

3 AUTHORS, INCLUDING:

Zhongfang Chen
University of Puerto Rico at Rio Piedras
220 PUBLICATIONS **7,854** CITATIONS

SEE PROFILE

Electron Attachment to the Hydrogenated Watson−Crick Guanine Cytosine Base Pair (GC+H): Conventional and Proton-Transferred Structures

J. David Zhang, Zhongfang Chen,† and Henry F. Schaefer*

Center for Computational Chemistry and Department of Chemistry, University of Georgia, Athens, GA 30602-2525

Received: December 20, 2007; Revised Manuscript Received: April 10, 2008

The anionic species resulting from hydride addition to the Watson−Crick guanine−cytosine (GC) DNA base pair are investigated theoretically. Proton-transferred structures of GC hydride, in which proton H1 of guanine or proton H4 of cytosine migrates to the complementary base-pair side, have been studied also. All optimized geometrical structures are confirmed to be minima via vibrational frequency analyses. The lowest energy structure places the additional hydride on the C6 position of cytosine coupled with proton transfer, resulting in the closed-shell anion designated **1T** ($G^-C(C6)$). Energetically, the major groove side of the GC pair has a greater propensity toward hydride/hydrogen addition than does the minor grove side. The pairing (dissociation) energy and electron-attracting ability of each anionic structure are predicted and compared with those of the neutral GC and the hydrogenated GC base pairs. Anion **8T** ($G(O6)C^-$) is a water-extracting complex and has the largest dissociation energy. Anion **2** ($GC(C4)^-$) and the corresponding open-shell radical GC(C4) have the largest vertical electron detachment energy and adiabatic electron affinity, respectively. From the difference between the dissociation energy and electron-removal ability of the normal GC anion and the most favorable structure of GC hydride, it is clear that one may dissociate the GC anion and maintain the integrity of the GC hydride.

Introduction

DNA damage caused by ionizing radiation has been of continuing interest in recent decades. Generated from simple ionization processes, electrons are the most abundant secondary species in the living cell.[1–13] Both experimental and theoretical studies have revealed that even low-energy electrons may attach to DNA nucleic acid bases (NABs) and induce either sugar-backbone σ-bond breakage or N1−glycosidic bond rupture (See Scheme 1 for IUPAC numbering scheme for the Watson−Crick guanine-cytosine (GC) base pair with backbones).[7,15–21] Furthermore, the radiation products of water, such as hydrogen atoms and hydroxl radicals, can react with charged NABs to cause base lesions. The stable lesion products, such as 8-oxo-guanine, resemble adenine instead of cytosine in the formation of mutagenic sequences.[22,23] If not repaired, a bad DNA sequence may be copied and translated to the next generation and cause potentially pathogenic cells. On the other hand, as a therapy to destroy tumor cells by damaging the cancerous DNA sequence, ionizing radiation can cause the demise of healthy cells. An always challenging question is whether one could find a substantial difference between the normal and damaged DNA sequence to design a medical radiation device to selectively break bad DNA molecules while keeping good species unchanged. Consequently, an understanding of differences in the molecular structures and electron-attracting abilities of both DNA normal subunits and geometrically altered subunits might be useful in the future in designing nanoscale medical devices.

To understand the electron-attracting ability of DNA subunits, the adiabatic electron affinities (AEAs) of these species should be determined. The valence-bound AEAs of individual NABs such as uracil (U), thymine (T), and cytosine (C) have been extrapolated from the AEAs of base−water clusters measured by photodetachment-photoelectron (PD-PE) spectroscopy.[24] Theoretical investigations have complemented experiments successfully, and experiment-consistent AEA values of the nucleobases, with the latest ordering U > T > C ≈ G (guanine) > A (adenine), have been confirmed by density functional theory (DFT) approaches.[25] Although the experimental determination of AEAs for the biologically related adenine−thymine (AT) and GC Watson−Crick base pairs still remains challenging, in 2005, Bowen and coworkers[26] reported the vertical detachment energy (VDE) of various AT and 9-methyladenine-1-methylthymine base pairs measured from photoelectron spectroscopy, in agreement with earlier theoretical predictions.[32] The canonical Watson−Crick base pairs AT and GC have been predicted by theory to have positive AEA values.[27–32] Recently, some disrupted DNA subunits, such as de-hydrogenated bases[33–35] and base pairs[36–38] and hydrogenated cytosine,[39–45] guanine,[46,47] and adenine,[48–53] have been detected experimentally, and the values of their AEAs have also been reported theoretically. The molecular structures of hydrogenated GC pairs have been reported recently,[54] whereas the AEA values have not been investigated yet. Meanwhile, it is well known that proton transfer (PT) plays an important role in stabilizing ionic DNA subunits upon radiation. Several theoretical studies have revealed that base pair anions are susceptible to PT.[55–58] It is thus important to consider PT structures in the present GC hydride study.

Here, we selected the hydrogenated Watson−Crick GC base pairs as models of damaged DNA base pair to explore AEAs and dissociation energies and to compare with those of the parent Watson−Crick GC pair.[31] The overall effect of electron attach-

* Corresponding author. E-mail: sch@uga.edu.
† Current address: Department of Physics, Applied Physics, and Astronomy, Rensselaer Polytechnic Institute, Troy, NY 12144.

10.1021/jp711958p CCC: $40.75
Published on Web 06/17/2008

SCHEME 1: GC Base Pair with Backbone

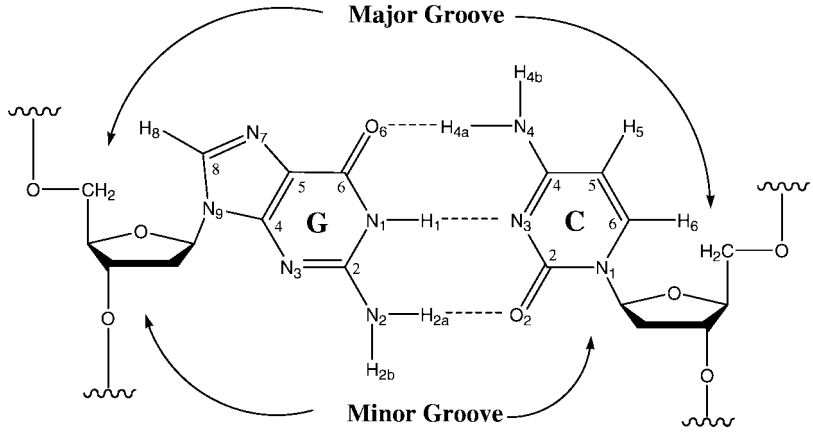

SCHEME 2: Reactions Associated with Hydrogen/ Electron Attachment to the GC Base Pair

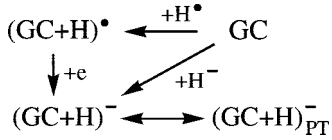

ment to hydrogenated GC is a hydride adding to each of the heavy atoms associated with seven double bonds of GC (reaction 1).

$$GC + H^- \rightarrow (GC + H)^- \quad (14 \text{ isomers}) \qquad (1)$$

$$(GC + H)^- \rightarrow (G + H)^- + C \text{ or } (C + H)^- + G \qquad (2)$$

We optimized the molecular structure of each isomer and predicted the dissociation energy associated with each structure (reaction 2). Each site-specific AEA has been obtained by evaluating the energy difference between the hydrogenated GC and the corresponding GC hydride, where a hydrogen atom has been attached to a different site of GC. Furthermore, we investigated significant PT reaction (reaction 3) of each hydride GC isomer and compared it with the PT process (reaction 4) for the GC anion. The product of reaction 3 is a complex of dihydrogenated guanine pairing with dehydrogenated cytosine anion ((G+2H)(C−H)⁻) or dehydrogenated guanine pairing with dihydrogenated cytosine ((G−H)⁻(C+2H)).

$$(GC + H)^- \rightarrow (G + 2H)(C - H)^- \text{ or } (G - H)^-(C + 2H) \qquad (3)$$

$$GC^- \rightarrow (G - H)^-(C + H) \qquad (4)$$

The geometrical structures of Watson−Crick GC⁻ and proton-transferred (G−H)⁻(C+H) are shown in Figure 1. Transition states for the reactions 3 and 4 have been located. Two possible PT pathways are found. In one pathway, the cytosine proton H4a transfers to guanine O6 (see Scheme 1 for numbering of atoms), where the anionic center resides on the guanine moiety. In the other pathway, the guanine H1 transfers to the N3 site of cytosine, where the anionic center is located on the cytosine moiety. Knowledge of the electronic characteristics of DNA subunits may be useful in building more biologically relevant models in order to develop future techniques for separating and repairing damaged DNA sequences.

Methods

Complete geometrical optimizations and vibrational frequency analyses were carried out by using DFT methods, specifically the B3LYP functional with DZP++ basis sets.[59] This combination has been demonstrated to provide reasonable theoretical results for DNA subunits.[31,32,36,37,54] The B3LYP method is a hybrid of the HF and DFT methods, incorporating Becke's three-parameter exchange functional (B3)[60] with the Lee, Yang, and Parr (LYP) correlation functional.[61] The DZP++ basis sets were constructed by augmenting the 1970 Huzinaga−Dunning contracted double-ζ basis with one set of five d-type polarization functions for each C, N, and O atom and a set of p functions on each H atom. In addition, even tempered s- and p-type diffuse functions were added to each C, N, and O, and a diffuse s function was added on each H. The final DZP++ set contains 19 functions per C, N, and O atom (10s6p1d/5s3p1d) and six functions per H (5s1p/3s1p).[62–64] Vibrational zero-point corrected relative energies and natural charges for the base pair were also determined by using the same approach. Numerical integrations were performed by using a fine grid of 75 radial and 302 angular points per shell.[65] Natural population atomic charges were determined by using the same level of theory with

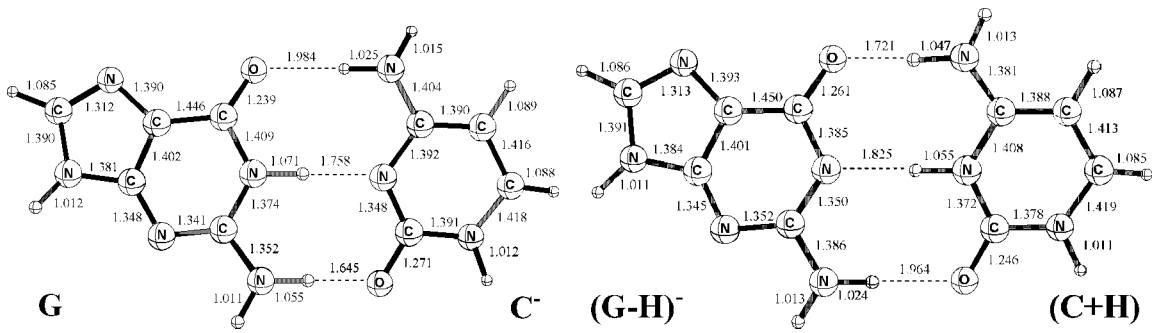

Figure 1. Optimized structures of non-proton-transferred GC base pair anions (GC⁻) and proton-transferred ((G−H)⁻(C+H)) anions. The unit of bond distance is the Angstrom.

TABLE 1: Zero-Point Vibrational Energy (ZPVE), Uncorrected and Corrected Relative Energies (kcal/mol) of Hydride GC Base Pair System

GC base pair hydride $(GC+H)^-$			GC base pair hydride with proton-transferred $(GC+H)^-_{PT}$		
anion structures	relative energies	relative energies (ZPVE corrected)	anion structures	relative energies	relative energies (ZPVE corrected)
1 $GC(C6)^-$	3.7	3.3	**1T** $G^-C(C6)$	0.0	0.0
2 $GC(C4)^-$	10.7	10.2	**2T** $G^-C(C4)$	5.3	5.8
	collapses to **3T**		**3T** $G(C6)C^-$	18.4	18.7
	collapses to **4T**		**4T** $G^-C(C2)$	22.0	22.0
5 $G(C2)^-C$	30.5	29.4		collapses to **5**	
6 $GC(C5)^-$	36.6	35.2	**6T** $G^-C(C5)$	37.1	35.7
	collapses to **7T**		**7T** $G(C4)C^-$	36.7	35.9
	collapses to **8T**		**8T** $G(O6)C^-$	42.3	40.6
9 $G(C8)^-C$	42.7	40.6	**9T** $G(C8)C^-$	39.7	38.4
10 $GC(N3)^-$	53.3	52.1			
11 $G(N7)^-C$	70.3	67.5	**11T** $G(N7)C^-$	69.9	67.7
12 $GC(O2)^-$	71.8	69.7	**12T** $G^-C(O2)$	61.2	59.4
13 $G(C5)^-C$	72.3	69.1	**13T** $G(C5)C^-$	71.4	69.2
14 $G(N3)^-C$	78.9	76.9		collapses to **14**	

TABLE 2: Dissociation Energies (D_e), Anion VDE, and AEAs of Radicals for GC and Hydrogenated/Hydride GC species[a]

GC base pair hydride				GC base pair hydride with proton transferred			
anion structures	D_e (kcal/mol)	VDE (eV)	AEA (eV)	anion structures	D_e (kcal/mol)	VDE (eV)	AEA (eV)
GC^-	39.4	1.20	0.44	$(G\text{-}H)^-(C+H)$	31.3	2.03	0.57
1 $GC(C6)^-$	40.1(27.7)	3.07	2.51	**1T** $G^-C(C6)$	28.9	3.39	3.18
2 $GC(C4)^-$	40.7(20.7)	4.03	3.45	**2T** $G^-C(C4)$	24.8	3.56	3.19
				3T $G(O6)C^-$	38.9(41.1)	3.31	2.85
				4T $G^-C(C2)$	21.5(27.2)	3.21	2.95
5 $G(C2)^-C$	13.5(14.8)	2.47	2.04				
6 $GC(C5)^-$	36.3(27.9)	1.64	0.99	**6T** $G^-C(C5)$	10.2	2.24	1.23
				7T $G(C4)C^-$	41.2(24.3)	2.85	1.58
				8T $G(O6)C^-$	49.1(19.7)	3.89	2.39
9 $G(C8)^-C$	21.9(28.1)	0.90	0.57	**9T** $G(C8)C^-$	45.2	1.64	0.70
10 $GC(N3)^-$	24.6(22.1)	1.46	0.24				
11 $G(N7)^-C$	23.7(25.9)	0.31	−0.16	**11T** $G(N7)C^-$	46.3	1.22	−0.14
12 $GC(O2)^-$	24.3(8.3)	1.36	0.52	**12T** $G^-C(O2)$	33.9	2.90	0.98
13 $G(C5)^-C$	12.2(23.8)	0.44	0.15	**13T** $G(C5)C^-$	12.2	1.52	0.19
14 $G(N3)^-C$	12.0(20.1)	1.21	0.23				

[a] The values inside parentheses are D_e for the corresponding neutral radicals at the same level of theory (from ref 54).

the natural bond order (NBO) analysis of Reed and Weinhold.[66–69] The GAUSSIAN 94 and 03 systems of DFT programs were used for the computations.[70]

Critical energetic properties were determined as follows.

AEA

$$\mathrm{AEA} = E(\text{optimized neutral}) - E(\text{optimized anion})$$

VDE

$$\mathrm{VDE} = E(\text{neutral at optimized anion geometry}) - E(\text{optimized anion})$$

Dissociation energy (DE)

$$\mathrm{DE} = E[(\mathrm{G}+\mathrm{H})-\mathrm{C}]^- - E(\mathrm{G}+\mathrm{H})^- - E(\mathrm{C})$$

or

$$\mathrm{DE} = E[\mathrm{G}-(\mathrm{C}+\mathrm{H})]^- - E(\mathrm{G}) - E(\mathrm{C}+\mathrm{H})^-$$

Results and Discussion

Hydrogenated and corresponding GC hydride structures have been selected herein as models to explore site-specific effects on damaged GC base pairs upon electron attachment. The formalism used to denote each hydrogenated/hydride GC structure is as follows. Addition of a hydrogen atom to one of the seven double bonds of the GC base pair, leading to open-shell radical structures, is denoted as $(GC+H)^\bullet$. There are a total of 14 open-shell structures thus generated. The analogous closed-shell anions were formed by incoming electron attachment to each of the 14 radicals; thus, the anions are denoted as $(GC+H)^-$. More anionic structures, denoted as $(GC+H)^-_{PT}$, should be considered because of PT processes triggered by electron attachment. The overall effect may be regarded as hydride addition to the GC base pair, as described by Scheme 2. The resulting anionic structures are specified by using G for the parent guanine and C for the parent cytosine, followed by the atom in which the hydrogen atom is appended in parentheses. Thus, $G(N3)^-C$ designates the anion generated by hydride addition to atom N3 of guanine, with the extra electron located on the G moiety; the corresponding PT structure of this anion is denoted as $G(N3)C^-$, explicitly indicating that the negative charge has migrated to the C moiety in the course of the PT process. Structures **1**−**14** illustrate each of the hydride GC base pairs, whereas the designations **1T**−**13T** label the corresponding PT structures.

SCHEME 3: Lewis Structures for 1 and 1T, Addressed by One of Reviewers of this Paper

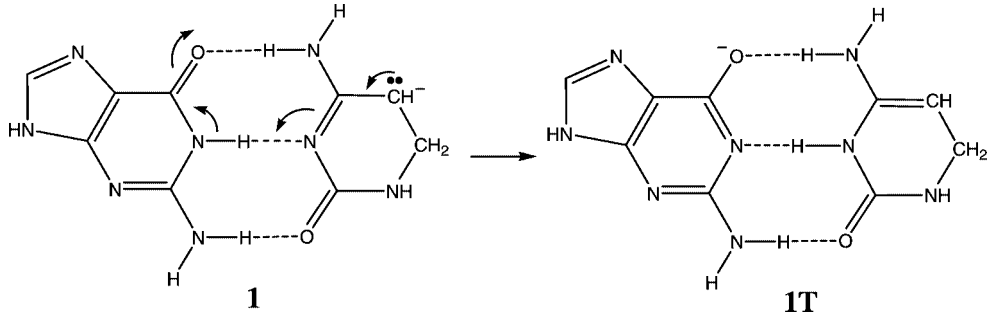

SCHEME 4: Energy Profiles for the PT, Electron Detachment, and Dissociation Reactions of (a) Structure 1 to 1T and (b) Structure 12 to 12T

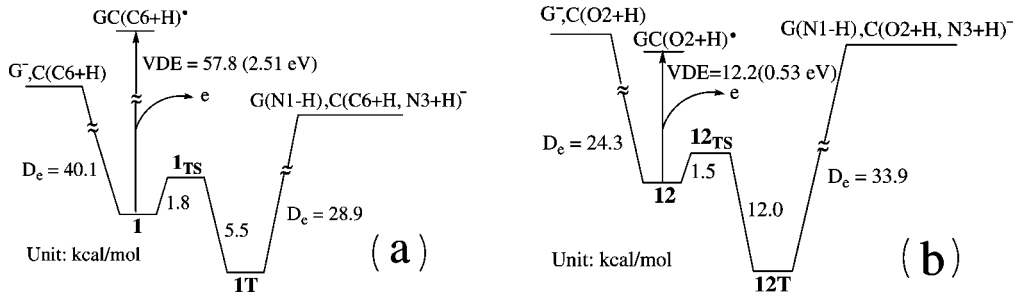

1. Energies and Geometries of GC Hydride Species. In Table 1, relative energies of $(GC+H)^-$ and $(GC+H)^-_{PT}$ are presented. The total energies are shown in the Supporting Information Table A. All structures are local minima on the potential energy surfaces as demonstrated via vibrational frequency computations (Figures 2–4). The formal anionic center has been marked in each structure. All optimized structures of $(GC+H)^-$ and $(GC+H)^-_{PT}$ deviate from the planar symmetry of the neutral GC base pair in the gas phase. Two dihedral angles $\tau(C6-N1)_G-(N3-C4)_C$ and $\tau(C6-C2)_G-(C2-C4)_C$ were selected as indicators of the effects of anion formation on the overall base pair geometries (see Supporting Information Table B).

There does not appear to be any systematic energetic preference in the addition of hydride to guanine rather than to the cytosine moiety. Among all isomers, PT structure **1T** with the hydride attached at cytosine C6 position has the lowest total energy. The non-PT structure **1** is predicted to lie only 3.7 kcal/mol above **1T**. Structure **2T,** denoted as $G^-C(C4)$, implies a PT structure from hydride addition to atom C4 of cytosine and lies 5.3 kcal/mol above the global minimum **1T**. Meanwhile, the non-PT structure **2**, denoted as $GC(C4)^-$, has a total energy 5.4 kcal/mol higher than that **2T**. In both structures **2** and **2T**, hydride addition leads to a tetrahedral cytosine C4 structure, which causes significant strain on the base pairing, reflected by large dihedral angle $\tau(C6-N1)_G-(N3-C4)_C$ (−12.5 and −14.0° for **2** and **2T**, respectively, Table B of the Supporting Information). The five structures with lowest free energies (**1T**, **1**, **2T**, **2**, and **3T**) are all formed by hydride addition on the major groove side of the GC double helix (Scheme 1). In the anionic structure **5** $(G(C2)^-C$, Figure 3), formation of a tetra-coordinated C2 atom reveals a loss of hydrogen-bonding ability with cytosine, consistent with earlier predictions for the G(C2)C radical.[54]

Unlike the radical structure G(O6)C,[54] the anion **8T** $(G(O6)C^-)$ is predicted to have an unprecedented structure (Figure 3), lying 42.3 kcal/mol higher than the global minimum **1T**. In this complex, a water molecule is formed, in which a hydride carbonyl group of guanine contributes OH and the amino group of cytosine provides an H atom. The negative charge in **8T** is mainly located at the dehydrogenated cytosine moiety, as indicated by both the Mulliken charge (−0.74 electrons) and the NBO charge (−0.86 electrons). However, structural analogues of **8**, **12**, and **12T** (Figure 3) have not been located as water-extracted complexes. The C2−O2 distances are 1.451 and 1.453 Å for **12** and **12T**, respectively, both significantly longer than that in the radical GC(O2) (1.371 Å)[54] but not sufficient for bond breakage.

Structure **10** $(GC(N3)^-$, Figure 4) lies 53.3 kcal/mol higher than **1T**, with a bifurcated hydrogen bond formed following hydride addition to N3 atom. There is an unusual hydrogen bond N2−H2···C2 in **12T** instead of the N2−H2···O2 in structure **12**. This may be because the cytosine C2 atom acquires substantial negative charge (−0.42 Mulliken electrons) as an anionic center at **12T**. Structure **14** is formed by addition of a hydride to the minor groove N3 atom of guanine. This structure has the highest total energy found for the $(GC+H)^-$ system, lying 78.9 kcal/mol above the global minimum **1T.** The PT structure for **14** was not found.

2. PT of GC Hydride Species. Not all $(GC+H)^-$ isomers have both PT and non-PT structures, for example, structures **3T**, **4T**, **7T**, **8T**, **10**, and **14**. However, if both exist, the PT structure has a lower total energy than the corresponding non-PT structure, except for **6T**. This phenomenon implies that PT molecular structures may be generally more favorable to attachment of an electron. There are possible explanations, but the underlying reason may be nontrivial. One such explanation, for which we are indebted to a thoughtful reviewer, follows. Simple Lewis structures (Scheme 3) for **1** and **1T** suggest that the guanine fragment in **1T** becomes more aromatic upon PT. The calculated bond lengths support this interpretation, with the N1−C6 bond shortening from **1** to **1T** and the C6−O6 bond lengthening from **1** to **1T**. The charge analysis described in Section 3 of our discussion could also be used to address such an interpretation. Perhaps an even simpler explanation is that

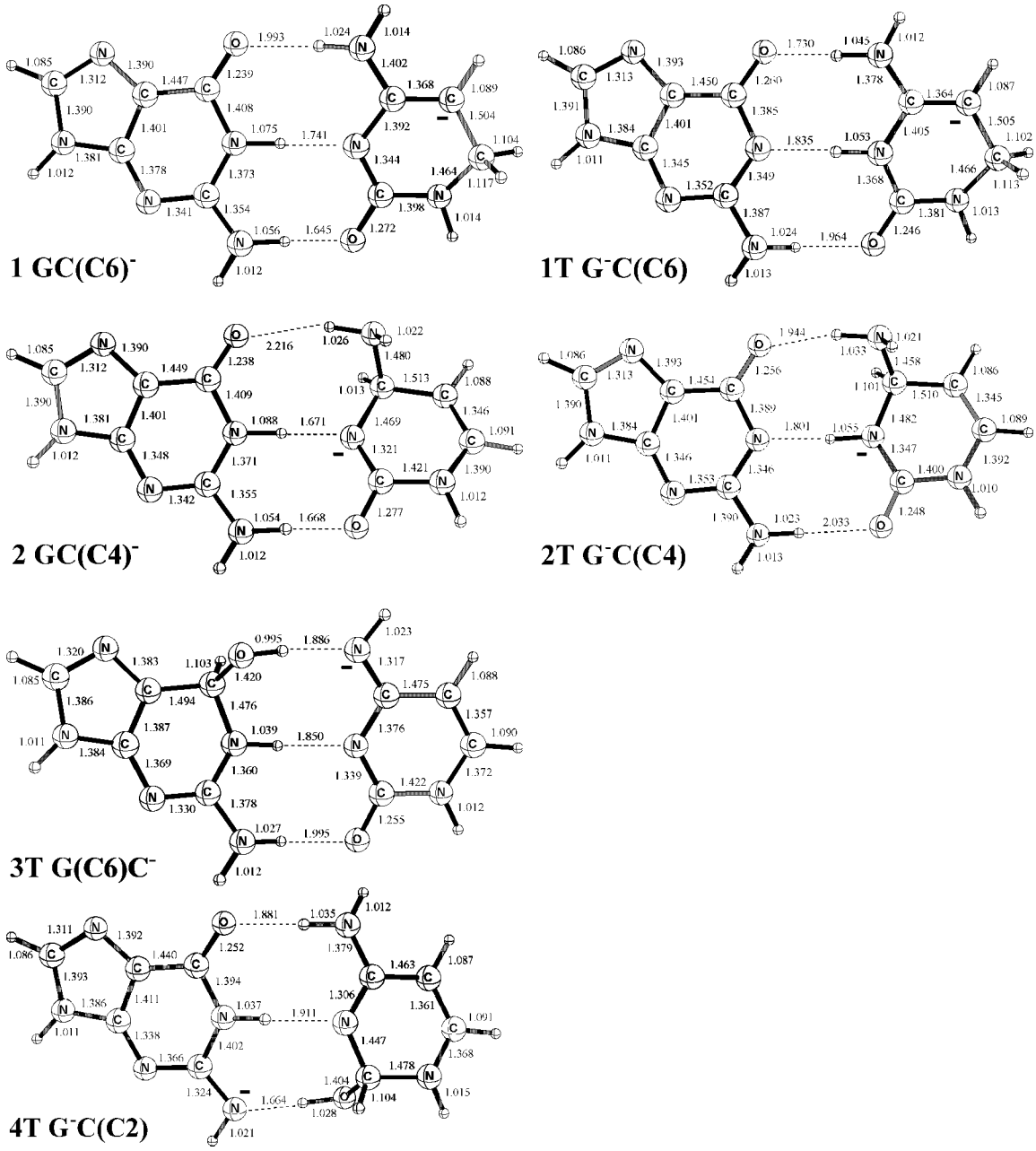

Figure 2. Optimized structures of GC hydrides from **1** to **4T**. A minus sign (−) shows the formal negative charge position. The unit of bond distance is the Angstrom.

1T allows the negative charge to be more localized on the more electronegative atom.

To understand the mechanism of the PT process, two transition states ($\mathbf{1_{TS}}$ and $\mathbf{12_{TS}}$) corresponding to two PT processes, **1** → **1T** and **12** → **12T**, respectively, were optimized. $\mathbf{1_{TS}}$ is probed because **1** and **1T** are the isomers with the lowest total energy. In contrast, **12** and **12T** have the largest energy difference (10.6 kcal/mol) among all PT/non-PT pairs. The energy profiles are shown in Scheme 4. Dissociation energies and vertical electron detachment energies are also included for comparison. The optimized structure of transition states is shown in Figure 5.

The $\mathbf{1_{TS}}$ vibrational analysis indicates that the imaginary vibrational frequency (1036i cm^{-1}) is the normal mode corresponding to the guanine N1−H1 stretching; in $\mathbf{12_{TS}}$, the analogous frequency is 1003i cm^{-1}. Two low energetic barriers are predicted, 1.8 kcal/mol for **1** → **1T** and 1.5 kcal/mol for **12** → **12T**. Compared to the higher dissociation energies and VDEs, these small barriers indicate that fast PT reactions may occur for **1** and **12**. The resulting PT products **1T** and **12T** are quite energetically favorable and thus may have long enough lifetimes to cause further DNA damage reactions before dissociation. For comparison, the barrier for the analogous PT reaction of the base pair radical anion GC^- is 2.3 kcal/mol at the same level of theor,[71] and 3.5 kcal/mol with the B3LYP/6-31+G(d) method.[56] The PT for the DNA nucleoside pair 2′-deoxyguanosine(dG)−2′-deoxycytidine(dC) anion also has been predicted to have a small barrier, 2.4 kcal/mol.[71]

3. Dissociation Energies. The dissociation energy discussed here is the energy required to separate the GC hydride pair into two monomers (guanine hydride + cytosine or cytosine hydride + guanine). For **8T**, dissociation leads to three monomers: deoxygened guanine + deprotonated cytosine + water molecule. There are some rules that should be noted from our findings.

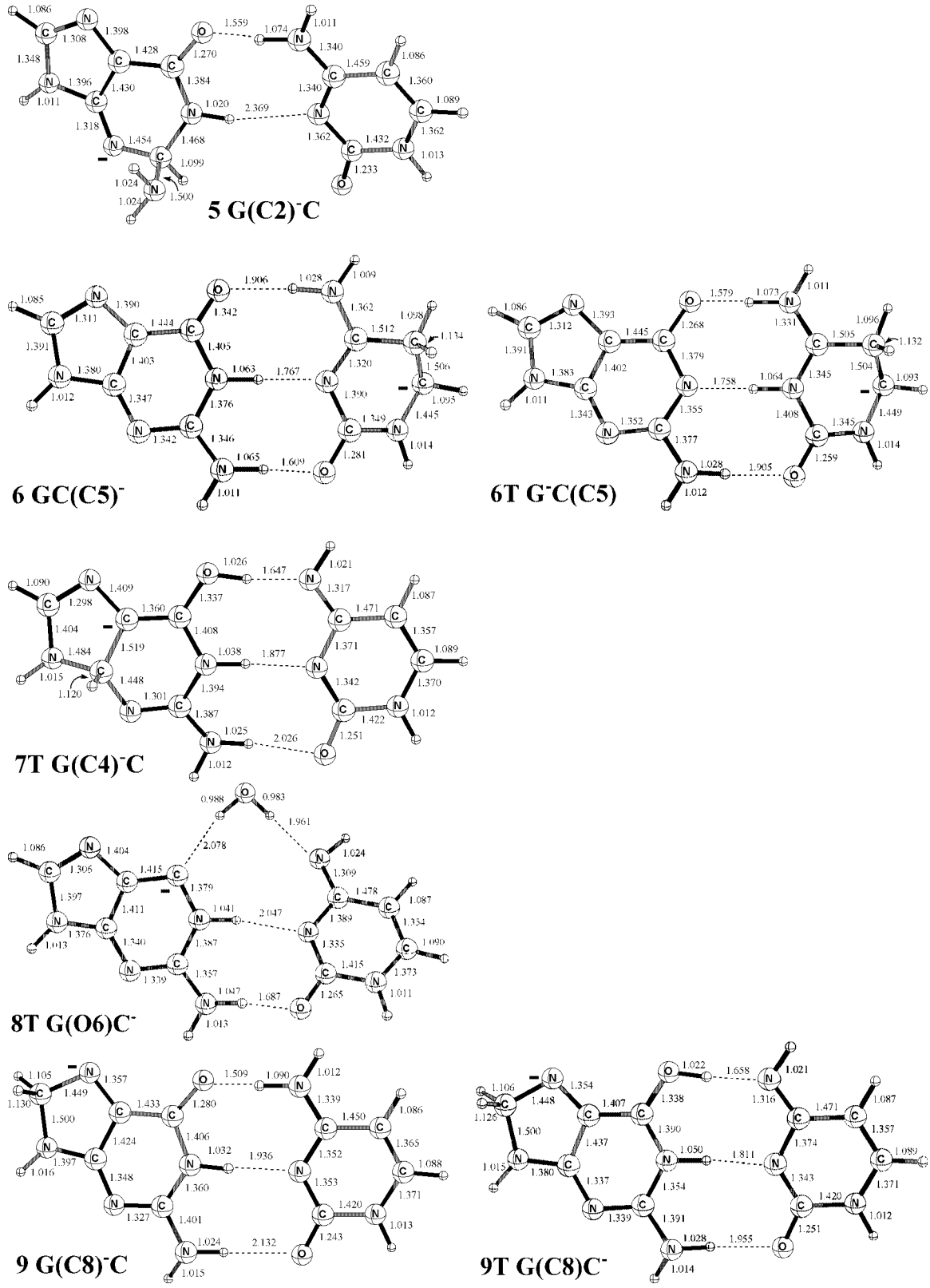

Figure 3. Optimized structures of GC hydrides from **5** to **9T**. A minus sign (−) shows the formal negative charge position. The unit of bond distance is the Angstrom.

Firstly, the more hydrogen bonds formed, the larger the predicted dissociation energy. For example, the complex structure **8T** has the largest D_e (49.1 kcal/mol, breaking four hydrogen bonds, Table 2), whereas **5** and **14** have quite low D_e values (both have two hydrogen bonds, with D_e = 13.5 and 12.0 kcal/mol, respectively, Table 2). Secondly, the formation of hydrogen bonds between two monomers may cause substantial strain for each of them. Hence, after dimer dissociation, the isolated monomer likely relaxes to the structure with the lowest free energy, thus decreasing the dissociation energy. For example, as the **6T** dissociation product (D_e = 10.2 kcal/mol), compound **15** is an energetically favored closed-shell structure (Figure 6), instead of the formal monomer of **6T** represented as a diradical structure of 3,5-dihydrogenated cytosine. Similarly, dissociation

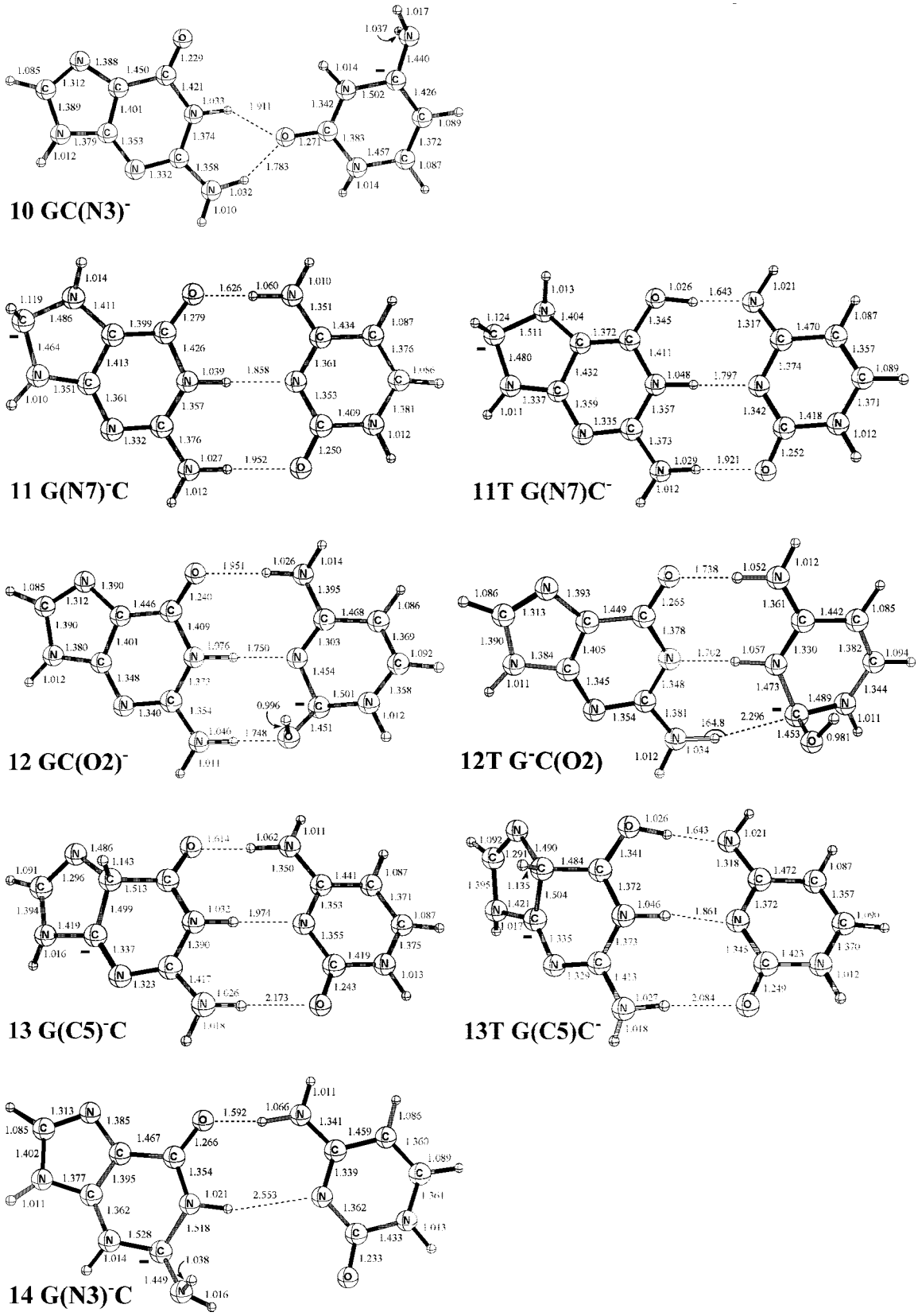

Figure 4. Optimized structures of GC hydrides from **10** to **14T**. A minus sign (−) shows the formal negative charge position. The unit of bond distance is the Angstrom.

of **13T** (D_e = 12.2 kcal/mol) yields a closed-shell structure **16** with a covalent bond forming between atoms C4 and C6 of the guanine moiety with two H atoms appended (Figure 6).

To separate a hydride GC pair, more energy is needed when the negative charge is primarily located on the cytosine part rather than on the guanine moiety. The average D_e for cytosine-centered anionic pairs is ∼36 kcal/mol, whereas it is ∼20 kcal/mol for guanine-centered pairs. Because of the higher AEAs of both cytosine and hydrogenated cytosine compared with those for the guanine derivatives,[31,45,47] this might be simply because

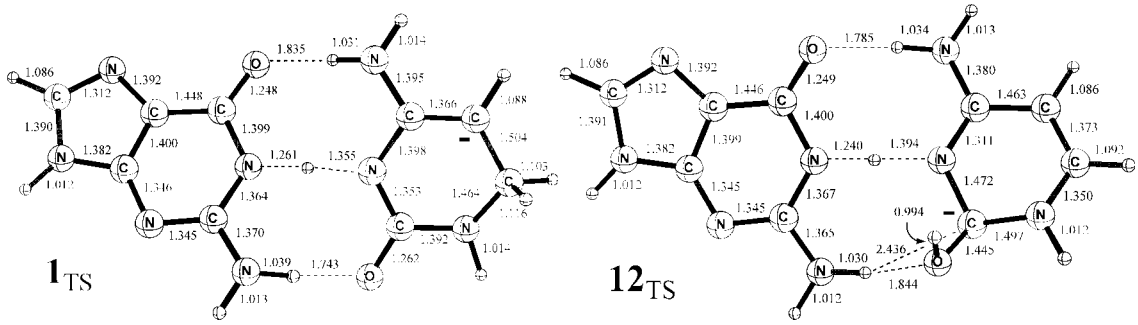

Figure 5. Optimized structures of transition states $\mathbf{1}_{TS}$ and $\mathbf{12}_{TS}$. A minus sign (−) shows the formal negative charge position. The unit of bond distance is the Angstrom.

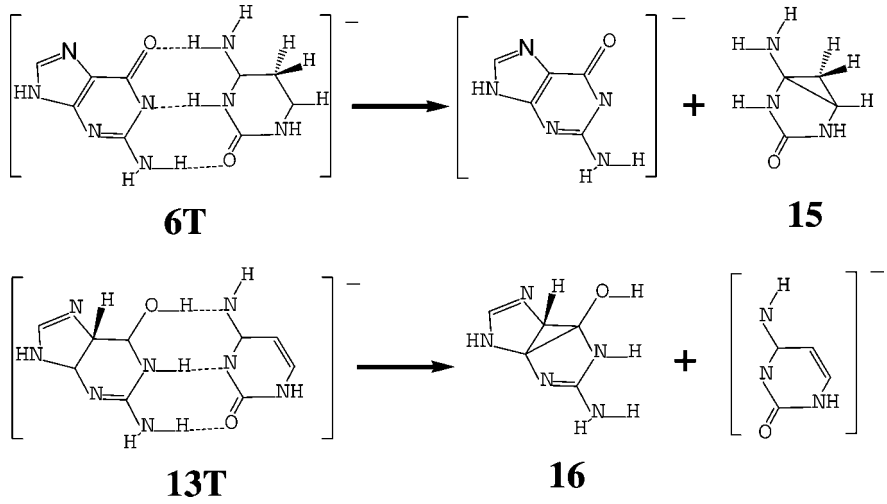

Figure 6. Dissociation reactions of structure **6T** and **13T**.

cytosine-centered anionic monomers have much lower total energies than those of guanine-centered monomers. In Table 2, one observes that the cytosine-centered anion GC^- is also predicted to have a larger D_e value than that of the corresponding guanine-centered PT structure $(G-H)^-(C+H)$ at the same theoretical level.

4. VDEs of GC Hydride and AEAs of Hydrogenated GC. All anionic structures of GC hydride have positive VDE values, ranging from 0.31 to 4.03 eV (Table 2). Generally, the PT anions have larger VDEs than the non-PT anions if both structures exist. Structure **2** has the largest VDE, indicating that the extra electron is least likely to be removed. The lowest total energy structure **1T** also has significant positive VDE (3.39 eV, 78.2 kcal/mol), which is much larger than the analogous D_e (28.9 kcal/mol), suggesting that anion **1T** may dissociate prior to ionization.

The predicted AEA values of hydrogenated GC (Table 2) are in the range from −0.16 to 3.45 eV. It may be interesting to compare the AEAs of (GC+H)• with those of the hydrogenated G (denoted as (G+H)•) and C (denoted as (C+H)•) monomers.[45,47] For hydride GC anions, if both non-PT and PT structures exist (Table 2), the higher AEA is selected and shown in Figure 7 with the AEAs of the isolated (G+H)• and (C+H)•. From Figure 7, the general trend of AEAs for (GC+H)• is consistent with those of isolated (G+H)• and (C+H)• systems. An exception occurs for G(O6), because the paired anion $G(O6)C^-$ has a complex structure with low free energy (Figure 3). Isolated (C+H)• radicals have lower AEAs than the corresponding paired (GC+H)• radicals. The AEAs of isolated (G+H)• and the corresponding paired (GC+H)• radicals display no clear pattern.

Conclusions

Hydride addition to the DNA Watson−Crick GC base pair generates 21 possible anionic structures. Generally, the proton-transferred structures have lower free energies compared to the non-PT structures. This can be understood in light of theoretical results for GC and dGdC. Anion **1T** has been predicted to be the global minimum. Considering the double-helix structure of the DNA sequence, hydride addition on the major grove side of the GC pair generates products with lower free energies than those generated on minor groove addition.

The AEAs of the hydrogenated GC radicals and the VDEs of the GC hydride anions range from −0.16 to 3.45 eV and from 0.31 eV to 4.03 eV, respectively. The wide range predicted in our theoretical studies implies complicated PD-PE spectra for GC hydride species. Among all species, structure **11** has the lowest VDE and the corresponding lowest AEA for its neutral radical.

The answer to the first question posed in the present paper (Can one find a substantial difference between the normal GC base pair and the hydrogenated GC under ionization radiation aimed to separate normal and damaged DNA sequences?) is positive. For example, the hydrogenated GC isomer with lowest free energy is structure G(C8)C (from ref 54), which has a very similar dissociation energy and AEA to the neutral Watson−Crick GC pair (ΔD_e = 0.9 kcal/mol and ΔAEA = 0.13 eV, Table 2). However, with the electron attachment from ionization radiation, **9T** ($G(C8)C^-$) differs substantially in energy from either GC^- or $(G-H)^-(C+H)$. For example, an energy of 40 kcal/mol is adequate to dissociate both GC^- and $(G-H)^-(C+H)$ (D_e values are 39.4 and 31.3 kcal/mol, respectively, Table 2). However,

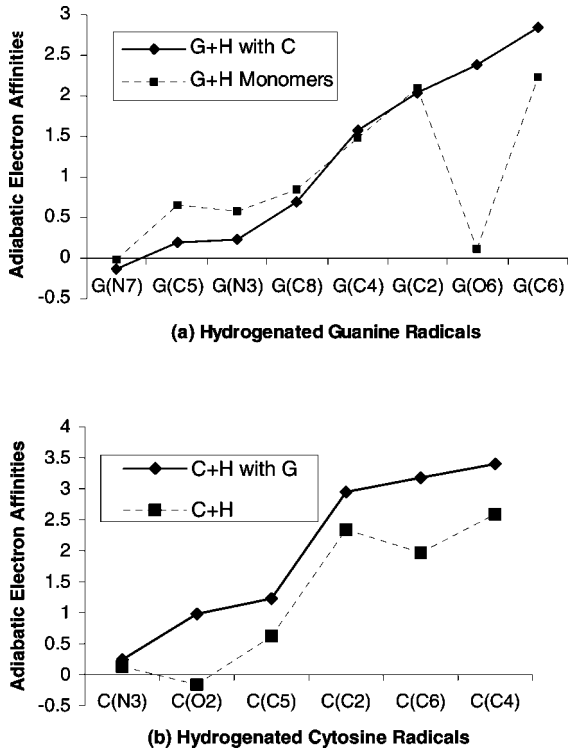

Figure 7. (a) Comparison of AEA predictions between the isolated (G+H) and the paired (G+H)C at the same level of theory. The AEA results for (G+H) are from ref 47. (b) Comparison of AEA predictions between the isolated (C+H) and the paired G(C+H) at the same level of theory. The AEA results for (C+H) are from ref 45.

this amount of energy is not sufficient to separate the base pair anion G(C8)C$^-$ (the latter D_e value is 45.2 kcal/mol, Table 2); instead, it is only enough to remove an electron from G(C8)C$^-$ (VDE value is 1.64 eV (37.8 kcal/mol), Table 2); thus, the G(C8)C$^-$ will remain bound.

Acknowledgment. This research was supported by the National Science Foundation, Grant CHE-0451445 and Grant CHE-0716718. Z.C. thanks the Research Computing Center (RCC) at the University of Georgia for providing computation facilities.

Supporting Information Available: This material is available free of charge via the Internet at http://pubs.acs.org.

References and Notes

(1) von Sonntag, C. *The Chemical Basis of Radiation Biology*; Taylor & Francis: New York, 1987.
(2) Becker, D.; Sevilla, M. D. *Advances in Radiation Biology*; Academic Press: New York, 1993.
(3) Colson, A. O.; Sevilla, M. D. *Int. J. Radiat. Biol.* **1995**, *67*, 627.
(4) Steenken, S. *Chem. Rev.* **1989**, *89*, 503.
(5) Steenken, S.; Telo, J. P.; Novais, H. M.; Candeias, L. P. *J. Am. Chem. Soc.* **1992**, *114*, 4701.
(6) Steenken, S.; Goldbergerova, L. *J. Am. Chem. Soc.* **1998**, *120*, 3928.
(7) Boudaiffa, B.; Cloutier, P.; Hunting, D.; Huels, M. A.; Sanche, L. *Science* **2000**, *287*, 1658.
(8) Li, X.; Sevilla, M. D.; Sanche, L. *J. Am. Chem. Soc.* **2003**, *125*, 13668.
(9) Caron, L. G.; Sanche, L. *Phys. Rev. Lett.* **2003**, *91*, 113201.
(10) Huels, M. A.; Boudaiffa, B.; Cloutier, P.; Hunting, D.; Sanche, L. *J. Am. Chem. Soc.* **2003**, *125*, 4446.
(11) Sanche, L. *Eur. Phys. J. D* **2005**, *35*, 367.
(12) Ptasińska, S.; Denifl, S.; Gohlke, S.; Scheier, P.; Illenberger, E.; Märk, T. D. *Angew. Chem., Int. Ed.* **2006**, *45*, 1893.
(13) Simons, J. *J. Acc. Chem. Res.* **2006**, *39*, 772.
(14) Barriors, R.; Skurski, P.; Simons, J. *J. Phys. Chem. B* **2002**, *106*, 7991.
(15) Berdys, J.; Ansiewicz, I.; Skurski, P.; Simons, J. *Acc. Chem. Res.* **2004**, *126*, 6441.
(16) Berdys, J.; Skurski, P.; Simons, J. *J. Phys. Chem. B* **2004**, *108*, 5800.
(17) Li, X.; Sanche, L.; Sevilla, M. D. *Radiat. Res.* **2006**, *165*, 721.
(18) Gu, J.; Wang, J.; Leszczynski, J. *J. Am. Chem. Soc.* **2006**, *128*, 9322.
(19) Gu, J.; Xie, Y.; Schaefer, H. F. *J. Am. Chem. Soc.* **2005**, *127*, 1053.
(20) Gu, J.; Xie, Y.; Schaefer, H. F. *J. Am. Chem. Soc.* **2006**, *128*, 1250.
(21) Bao, X.; Wang, J.; Gu, J.; Leszcynski, J. *Proc. Nat. Acad. Sci. U.S.A.* **2006**, *103*, 5658.
(22) Malins, D. C.; Polissar, N. L.; Ostrander, G. K.; Vinson, M. A. *Proc. Natl. Acad. Sci. U.S.A.* **2000**, *97*, 12442.
(23) Cheng, X.; Kelso, C.; Hornak, V.; de los Santos, C.; Grollman, A. P.; Simmerling, C. *J. Am. Chem. Soc.* **2005**, *127*, 13906.
(24) Schiedt, J.; Weinkauf, R.; Neumark, D. M.; Schlag, E. W. *Chem. Phys.* **1998**, *239*, 511.
(25) Wesolowski, S. S.; Leininger, M. L.; Pentchev, P. N.; Schaefer, H. F. *J. Am. Chem. Soc.* **2001**, *123*, 4023.
(26) Radisic, D.; Bowen, K. H.; Dabkowska, I.; Storoniak, P.; Rak, J.; Gutowski, M. *J. Am. Chem. Soc.* **2005**, *127*, 6443.
(27) Li, X.; Cai, Z.; Sevilla, M. D. *J. Phys. Chem. B* **2001**, *105*, 10115.
(28) Li, X.; Cai, Z.; Sevilla, M. D. *J. Phys. Chem. A* **2002**, *106*, 9345.
(29) Li, X.; Sevilla, M. D.; Sanche, L. *J. Am. Chem. Soc.* **2003**, *125*, 8916.
(30) Reynisson, J.; Steenken, S. *Phys. Chem. Chem. Phys.* **2002**, *4*, 5353.
(31) Richardson, N. A.; Wesolowski, S. S.; Schaefer, H. F. *J. Am. Chem. Soc.* **2002**, *124*, 10163.
(32) Richardson, N. A.; Wesolowski, S. S.; Schaefer, H. F. *J. Phys. Chem. B* **2003**, *107*, 848.
(33) Liu, B.; Hvelplund, P.; Nielsen, S. B.; Tomita, S. *J. Chem. Phys.* **2004**, *121*, 4175.
(34) Denifl, S.; Ptasinska, S.; Probst, M.; Hrusak, J.; Scheier, P.; Mark, T. D. *J. Phys. Chem. A* **2004**, *108*, 6562.
(35) Abdoul-Carime, H.; Langer, J.; Huels, M. A.; Illenberger, E. *Eur. Phys. J. D* **2005**, *35*, 399.
(36) Bera, P. P.; Schaefer, H. F. *Proc. Natl. Acad. Sci. U.S.A.* **2005**, *102*, 6698.
(37) Lind, M. C.; Bera, P. P.; Richardson, N. A.; Wheeler, S. E.; Schaefer, H. F. *Proc. Natl. Acad. Sci. U.S.A.* **2006**, *103*, 7554.
(38) Lind, M. C.; Richardson, N. A.; Wheeler, S. E.; Schaefer, H. F. *J. Phys. Chem. B* **2007**, *111*, 5525.
(39) Colson, A. O.; Becker, D.; Eliezer, I.; Sevilla, M. D. *J. Phys. Chem. A* **1997**, *101*, 8935.
(40) Debije, M. D.; Bernhard, W. A. *J. Phys. Chem. A* **2002**, *106*, 4608.
(41) Debije, M. G.; Close, D. M.; Bernhard, W. A. *Radiat. Res.* **2002**, *157*, 235.
(42) Turecek, F.; Yao, C. *J. Phys. Chem. A* **2003**, *107*, 9221.
(43) Chen, X.; Syrstad, E. A.; Nguyen, M. T.; Gerbaux, P. G.; Turecek, F. *J. Phys. Chem. A* **2005**, *109*, 8121.
(44) Yao, C.; Cuadrado-Peinado, M. L.; Polasek, M.; Turecek, F. *Angew. Chem., Int. Ed.* **2005**, *44*, 6708.
(45) Zhang, J. D.; Xie, Y.; Schaefer, H. F.; Luo, Q.; Li, Q.-S. *Mol. Phys.* **2006**, *104*, 2347.
(46) Wetmore, S. D.; Boyd, R. J.; Eriksson, L. A. *J. Phys. Chem. B* **1998**, *102*, 9332.
(47) Zhang, J. D.; Xie, Y.; Schaefer, H. F. *J. Phys. Chem. A* **2006**, *110*, 12010.
(48) Lichter, J. J.; Gordy, W. *Proc. Natl. Acad. Sci. U.S.A.* **1968**, *60*, 450.
(49) Close, D. M.; Nelson, W. H.; Sagstuen, E.; Hole, E. O. *Rad. Res.* **1994**, *137*, 309.
(50) Colson, A. O.; Sevilla, M. D. *J. Phys. Chem.* **1995**, *99*, 13037.
(51) Colson, A. O.; Becker, D.; Eliezer, I.; Sevilla, M. D. *J. Phys. Chem. A* **1997**, *101*, 8941.
(52) Wetmore, S. D.; Boyd, R. J.; Eriksson, L. A. *J. Phys. Chem. B* **1998**, *102*, 10614.
(53) Reynisson, J.; Steenken, S. *Phys. Chem. Chem. Phys.* **2005**, *7*, 665.
(54) Zhang, J. D.; Schaefer, H. F. *J. Chem. Theory Comput.* **2007**, *3*, 115.
(55) Colson, A. O.; Besler, B.; Close, D. M.; Sevilla, M. D. *J. Phys. Chem.* **1992**, *96*, 661.
(56) Li, X.; Cai, Z.; Sevilla, M. D. *J. Phys. Chem. B* **2001**, *105*, 10115.
(57) Gorb, L.; Podolyan, Y.; Dziekonski, P.; Sokalski, W. A.; Leszczynski, J. *J. Am. Chem. Soc.* **2004**, *126*, 10119.
(58) Zoete, V.; Meuwly, M. *J. Chem. Phys.* **2004**, *121*, 4377.
(59) Rienstra-Kiracofe, J. C.; Tschumper, G. S.; Schaefer, H. F.; Nandi, S.; Ellison, G. B. *Chem. Rev.* **2002**, *102*, 231.
(60) Becke, A. D. *J. Chem. Phys.* **1993**, *98*, 5648.
(61) Lee, C.; Yang, W.; Parr, R. G. *Phys. Rev. B* **1988**, *37*, 785.
(62) Huzinaga, S. *J. Chem. Phys.* **1965**, *42*, 1293.
(63) Dunning, T. H. *J. Chem. Phys.* **1970**, *53*, 2823.
(64) Lee, T. J.; Schaefer, H. F. *J. Chem. Phys.* **1985**, *83*, 1784.

(65) Papas, B. N.; Schaefer, H. F. *J. Mol. Struct.* **2006**, *768*, 175.
(66) Reed, A. E.; Weinstock, R. B.; Weinhold, F. *J. Chem. Phys.* **1985**, *83*, 735.
(67) Reed, A. E.; Weinhold, F. *J. Chem. Phys.* **1985**, *83*, 1736.
(68) Reed, A. E.; Curtiss, L. A.; Weinhold, F. *Chem. Rev.* **1988**, *88*, 899.
(69) Reed, A. E.; Schleyer, P. R. *J. Am. Chem. Soc.* **1990**, *112*, 1434.
(70) (a) Frisch, M. J.; Trucks, G. W.; Schlegel, H. B.; Gill, P. M. W.; Johnson, B. G.; Robb, M. A.; Cheeseman, J. R.; Keith, T.; Petersson, G. A.; Montgomery, J. A.; Raghavachari, K.; Al-Laham, M. A.; Zakrzewski, V. G.; Ortiz, J. V.; Foresman, J. B.; Cioslowski, J.; Stefanov, B. B.; Nanayakkara, A.; Challacombe, M.; Peng, C. Y.; Ayala, P. Y.; Chen, W.; Wong, M. W.; Andres, J. L.; Replogle, E. S.; Gomperts, R.; Martin, R. L.; Fox, D. J.; Binkley, J. S.; Defrees, D. J.; Baker, J.; Stewart, J. P.; Head-Gordon, M.; Gonzalez, C.; Pople, J. A. *Gaussian 94*, revision B.3; Gaussian, Inc.: Pittsburgh, PA, 1995. (b) Frisch, M. J.; Trucks, G. W.; Schlegel, H. B.; Scuseria, G. E.; Robb, M. A.; Cheeseman, J. R.; Montgomery, J. A., Jr.; Vreven, T.; Kudin, K. N.; Burant, J. C.; Millam, J. M.; Iyengar, S. S.; Tomasi, J.; Barone, V.; Mennucci, B.; Cossi, M.; Scalmani, G.; Rega, N.; Petersson, G. A.; Nakatsuji, H.; Hada, M.; Ehara, M.; Toyota, K.; Fukuda, R.; Hasegawa, J.; Ishida, M.; Nakajima, T.; Honda, Y.; Kitao, O.; Nakai, H.; Klene, M.; Li, X.; Knox, J. E.; Hratchian, H. P.; Cross, J. B.; Bakken, V.; Adamo, C.; Jaramillo, J.; Gomperts, R.; Stratmann, R. E.; Yazyev, O.; Austin, A. J.; Cammi, R.; Pomelli, C.; Ochterski, J. W.; Ayala, P. Y.; Morokuma, K.; Voth, G. A.; Salvador, P.; Dannenberg, J. J.; Zakrzewski, V. G.; Dapprich, S.; Daniels, A. D.; Strain, M. C.; Farkas, O.; Malick, D. K.; Rabuck, A. D.; Raghavachari, K.; Foresman, J. B.; Ortiz, J. V.; Cui, Q.; Baboul, A. G.; Clifford, S.; Cioslowski, J.; Stefanov, B. B.; Liu, G.; Liashenko, A.; Piskorz, P.; Komaromi, I.; Martin, R. L.; Fox, D. J.; Keith, T.; Al-Laham, M. A.; Peng, C. Y.; Nanayakkara, A.; Challacombe, M.; Gill, P. M. W.; Johnson, B.; Chen, W.; Wong, M. W.; Gonzalez, C.; Pople, J. A. *Gaussian 03*; Gaussian, Inc.: Wallingford, CT, 2004.
(71) Gu, J.; Xie, Y.; Schaefer, H. F. *J. Chem. Phys.* **2007**, *127*, 155107.

JP711958P